Institute for the Theory of Advanced Materials in Information Technology

(DMR-0325218)

Walter Library, Digital Technology Center at the University of Minnesota

Mission:

The Institute is dedicated to promoting research on understanding and predicting the properties of materials used in information technology.

http://www.itamit.dtc.umn.edu/

Jim Chelikowsky and Yousef Saad
University of Minnesota

Organization

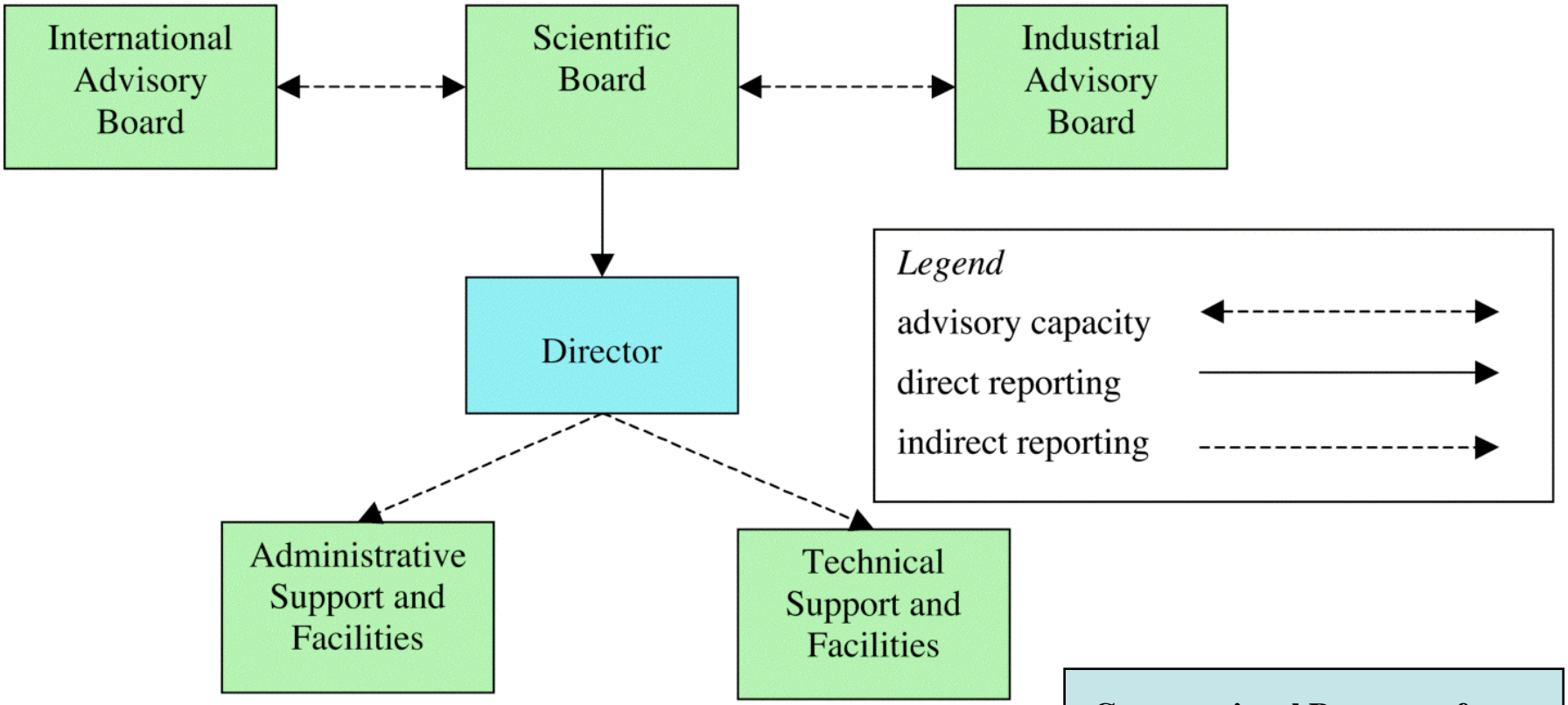

Computational Resources from the Minnesota Supercomputing Institute

Science Board

Yousef Saad
University of Minnesota

Jim Chelikowsky
University of Minnesota

Steve Louie
UC Berkeley

Renata Wentzcovitch
University of Minnesota

Efthimios Kaxiras
Harvard University

Andreas Stathopoulos
William and Mary

Industrial Board

Dr. James Chadi, Chief Scientist, Science Division, NEC
Dr. Ken Hass, Manager, Chemistry & Environmental Science Department, Ford Motor Company
Dr. Alex Demkov, Principal Staff Scientist, Motorola Physical Sciences Research Laboratories
Dr. Doug Allan, Research Associate, Corning
Dr. Cristina Thomas, Senior Research Specialist, 3M
Dr. John R. Smith, Group Manager, Manufacturing Processes Research, Delphi Automotive Systems
Dr. Gaddi Haase, Staff Scientist, Texas Instruments
Drs. Y.-K. Kwon and S.-H. Jhi, Nanomix
Dr. Sadas Shankar, Intel

International Board

Professor Achi Brandt (Weizmann Institute of Science, Rehovoth Israel)
Dr. Nadia Binggeli (International Center for Theoretical Physics, Trieste, Italy)
Dr. Leeor Kronik (Weizmann Institute of Science, Rehovoth, Israel)
Professor Jose Luis Martins (Instituto Superior Tecnico, Lisbon, Portugal)
Professor Angel Rubio (University Pais Vasco, San Sebastian/Donostia, Spain)
Professor Matthias Scheffler (Max Planck Institute, Berlin Germany)

Outreach and Education Activities

European Commision/National Science Foundation Workshop on "Computational Methods in Materials Science." San Francisco, April 15 and 16. Report:

http://www-itamit-test.dtc.umn.edu/nsfreport.php

Coordination Meeting: August 6 and 7 (Science, Industrial and International Boards)

Software link:

http://www.itamit.dtc.umn.edu/software.html

Summer Intern Program:
Eric Lindgren
Carleton College

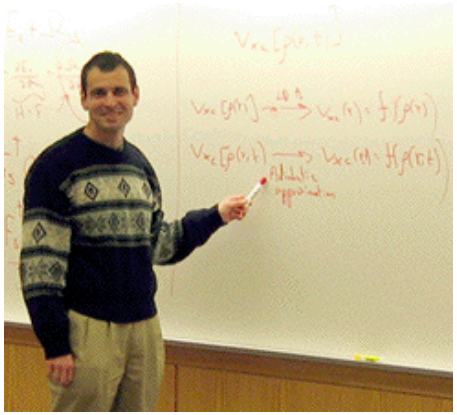

Visitors: Leeor Kronik and Adi Makmal from the Weizmann Institute

Postdocs/Students

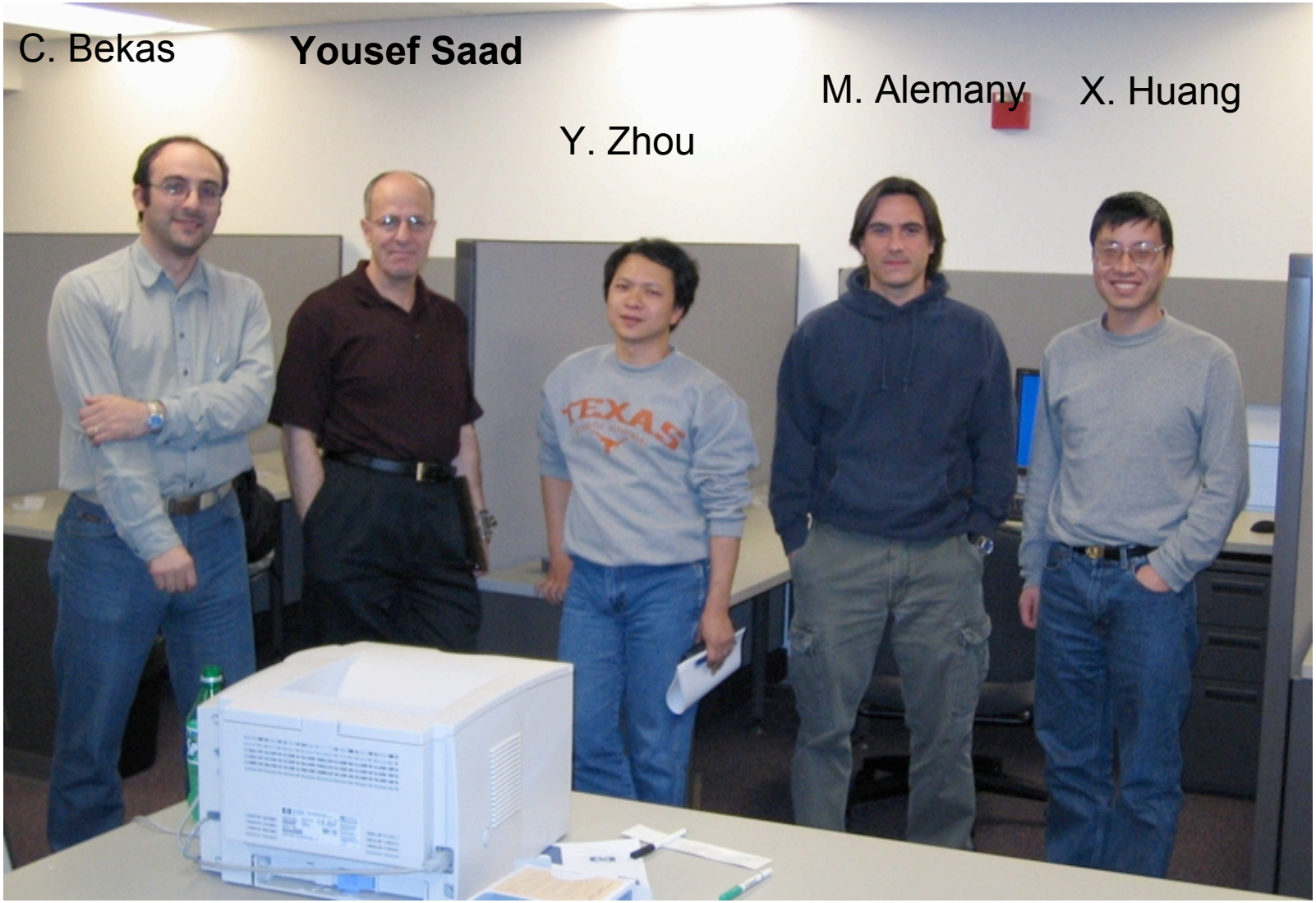

Lingzhu Kong

Marié López del Puerto

Shiv Gowda

Shen Li

Chemical Engineering, Chemical Physics, Materials Science, Physics, Scientific Computation and Computer Science

One of the greatest accomplishments of humankind: Changing silicon from beach sand to the the stuff of supercomputers

Heading toward the nanoscale.....

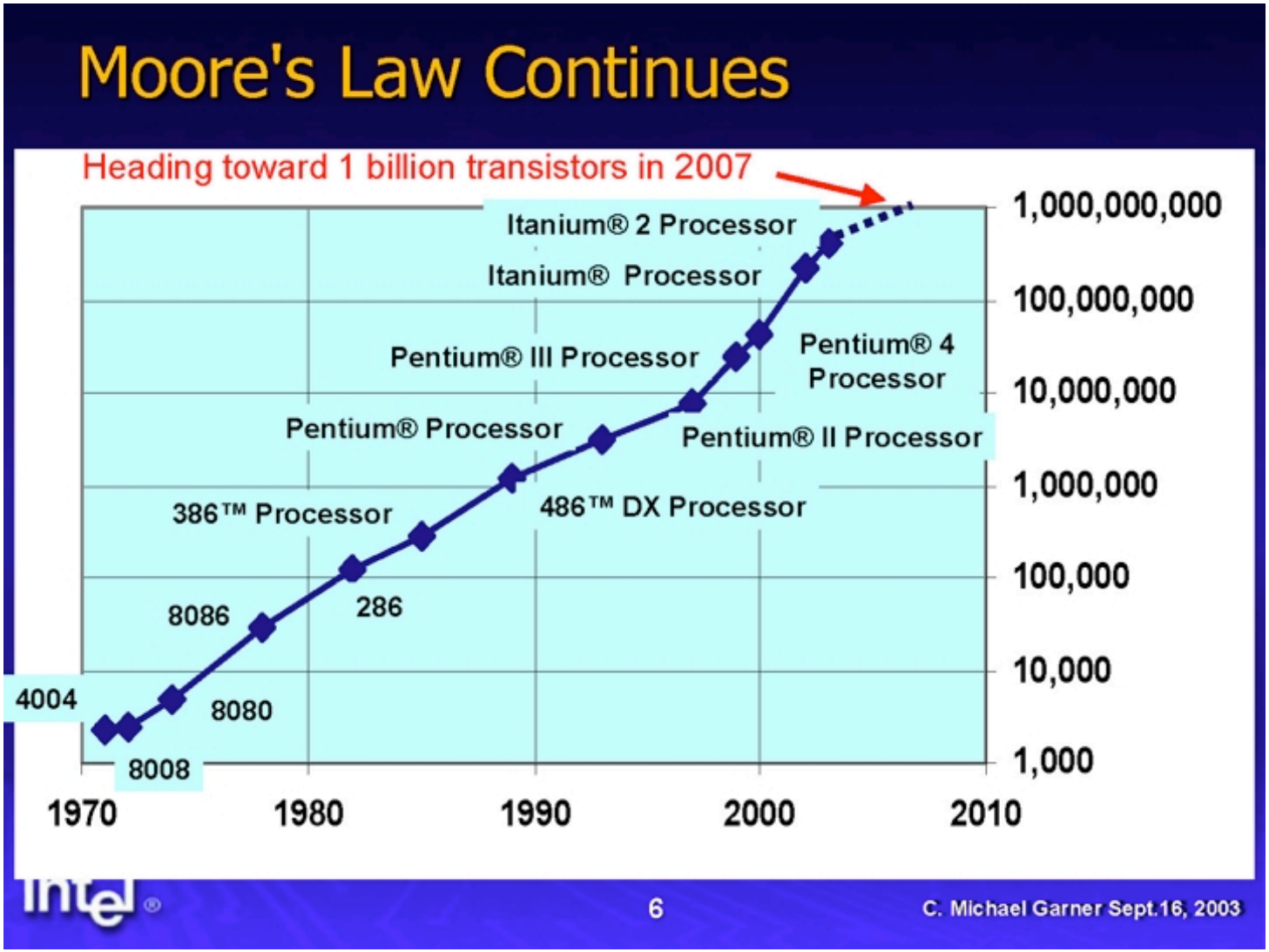

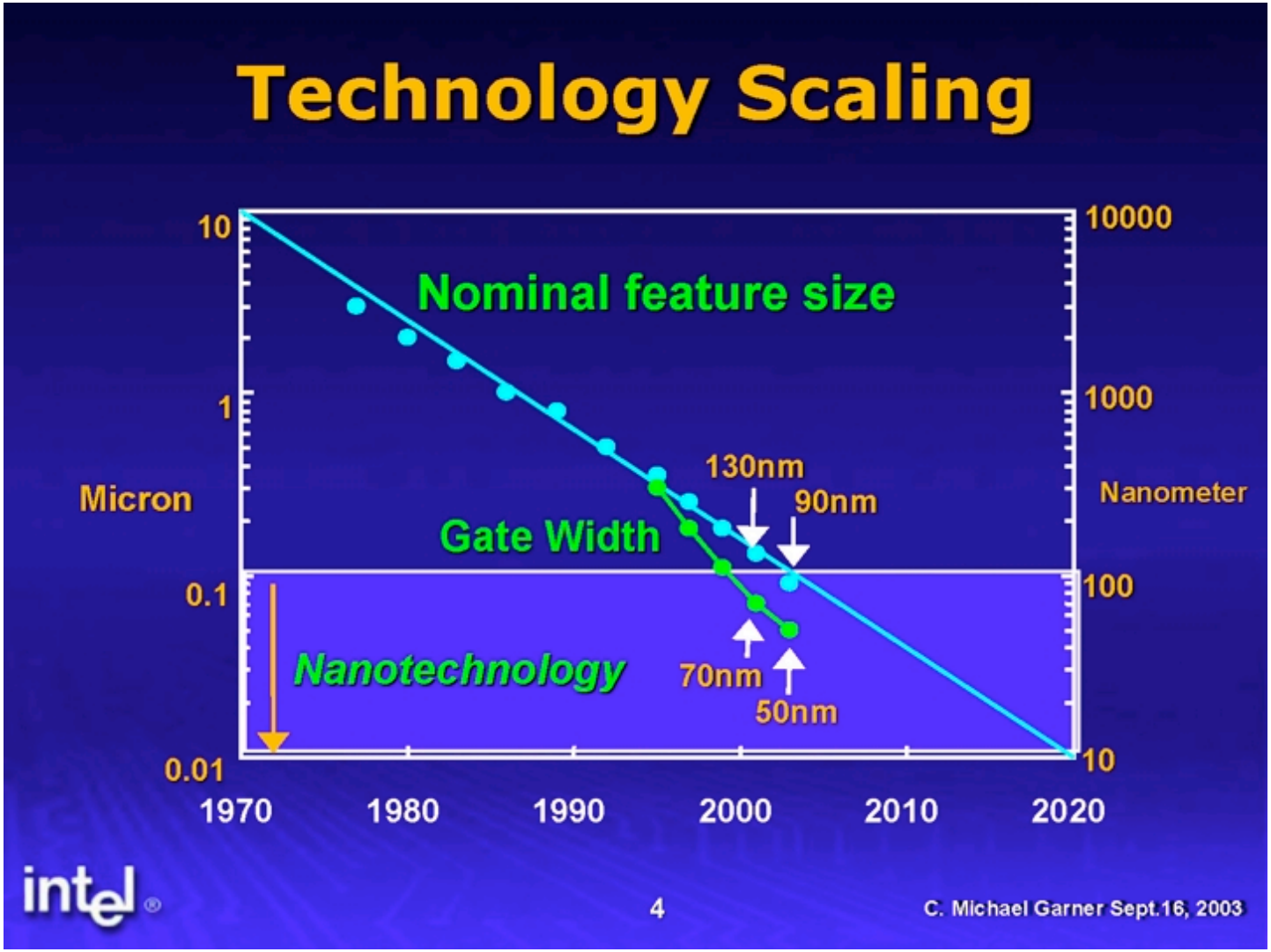

Intel is now a "nanotechnology company."

Examples of Materials of Interest to Intel....

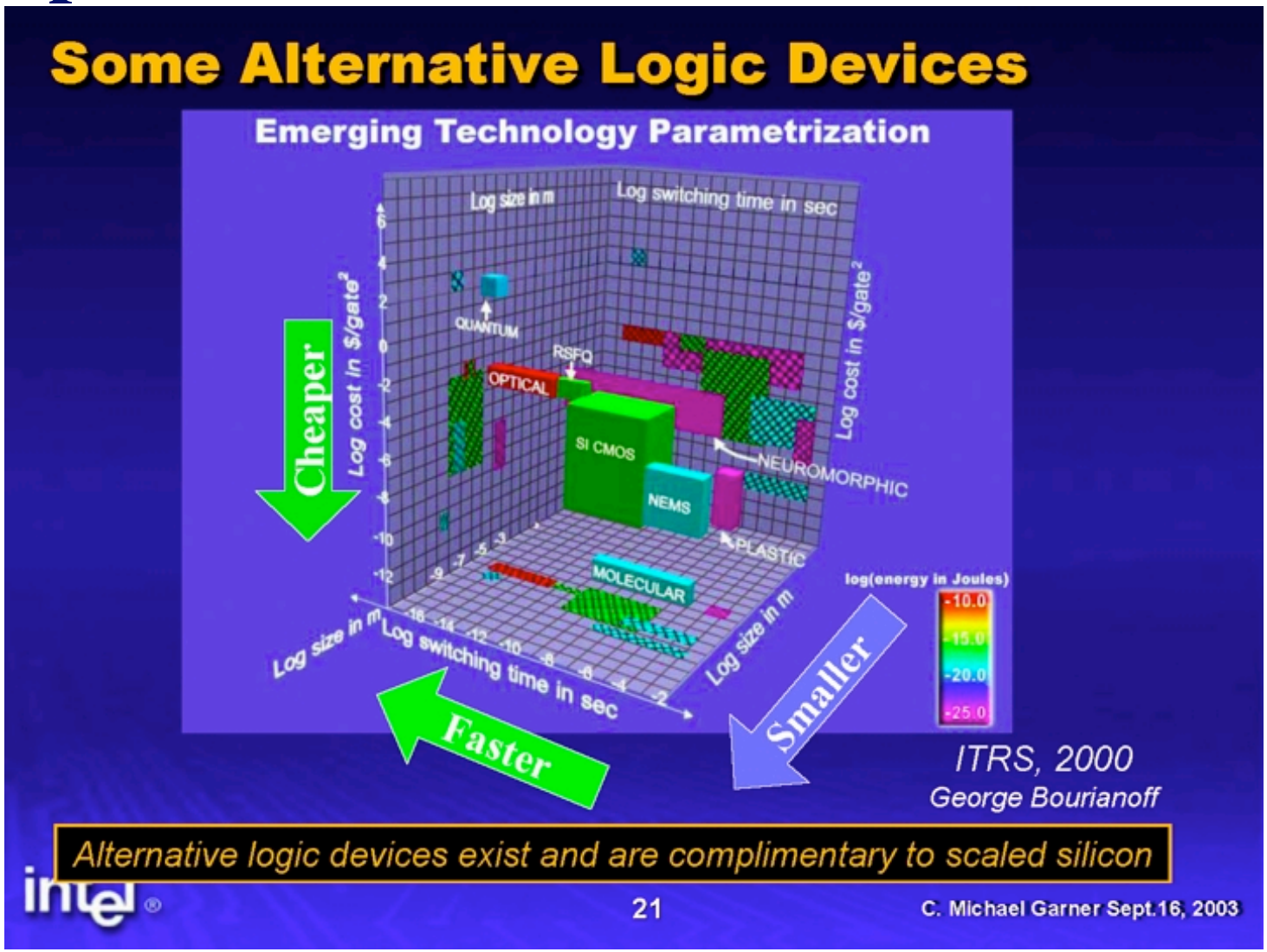

One acre of silicon wafers is worth one billion dollars.--F. Seitz

Research Programs

Dielectrics: Defects in silica
Clusters and quantum dots:
Optical, structural and magnetic properties

⇦ POSTERS

Surfaces: Adsorption, defects and growth
Liquids: Microstructure, growth
Organic semiconductors and nanotubes

⇦ Web Site

Molecular electronics
Spintronic materials:
- **$Co_{1-x}Fe_xS_2$ half metals**
- **Growth of Mn:Ge Surfaces**
- **Mn:ZnSe Quantum dots**

High performance algorithms

Molecular Electronics

(Electron transport through single molecules, atomic wires, …)

- Developed a new approach based on an *ab initio* scattering-state method
- Applied to nonlinear I-V studies of molecular junctions, atomic wires, nanotubes

Son, Choi, Ihm, Cohen, and Louie

First-principles Scattering-State Approach to Molecular Electronic Devices

- Prototype: a molecule between two metal probes.

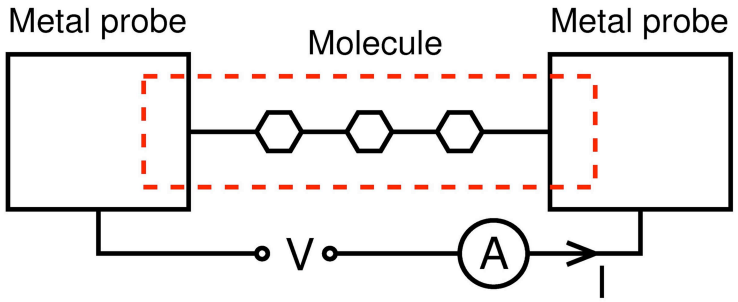

- Chemical potentials in the two probes are different by bias voltage.
- The Kohn-Sham potential near the molecule is calculated self-consistently.
- Current is obtained from the integration of transmission coefficients between chemical potentials.

$$I(V) = \frac{2e}{h} \int_{\mu_R}^{\mu_L} T(E,V)dE$$

I-V Characteristics of Electron Transport through a Tour (polyphenylene-based chains) Molecule

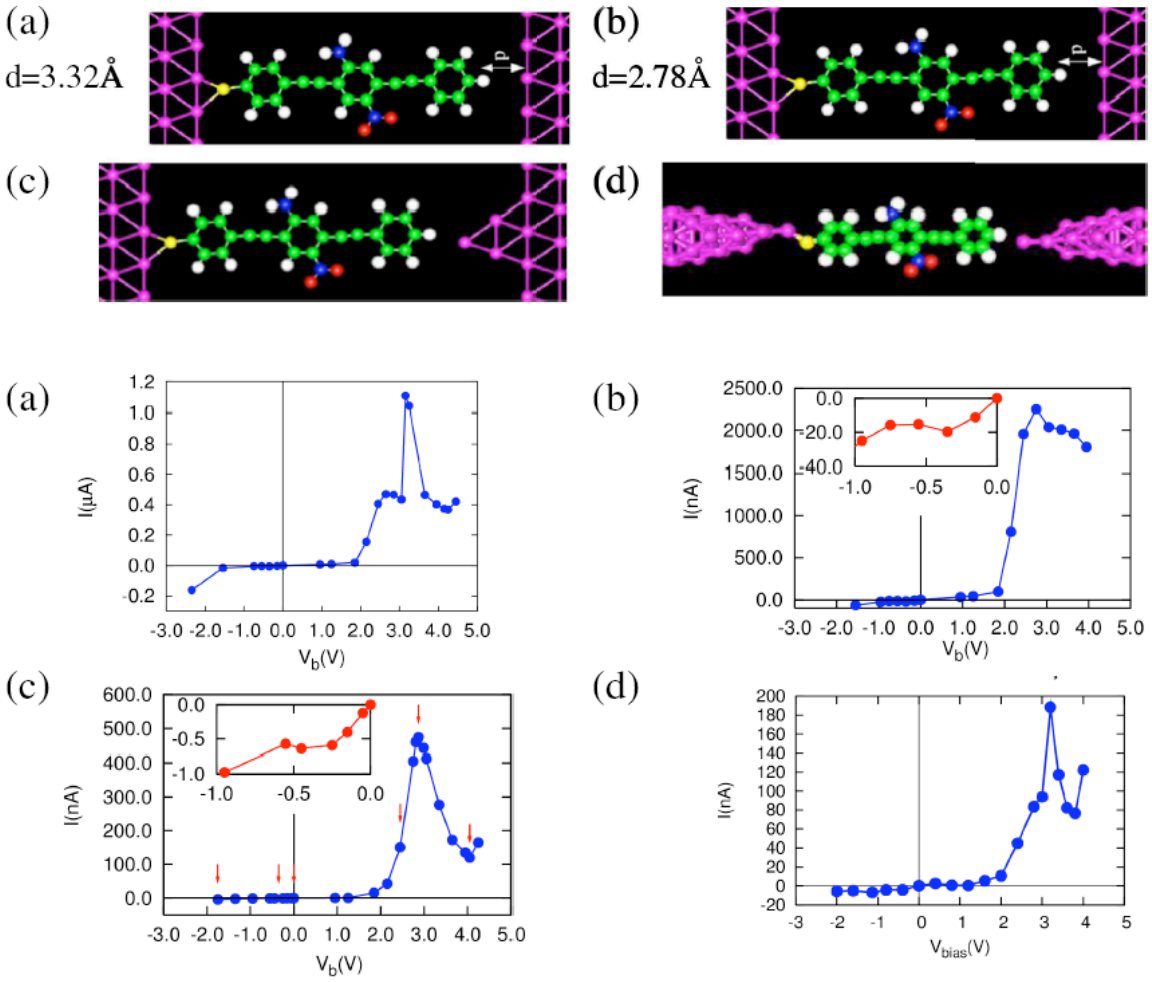

- Large negative differenential resistance
- Strong sensitivity to contact geometry

Spintronics

Can we "inject spin" into electronic devices?
Spintronics !!

e.g., The spinFET

Datta & Das, APL, 1990

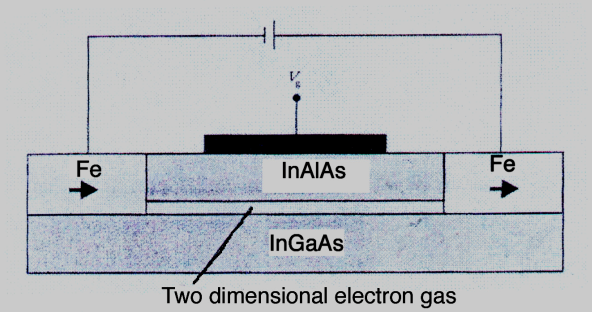

The spin valve – a memory element

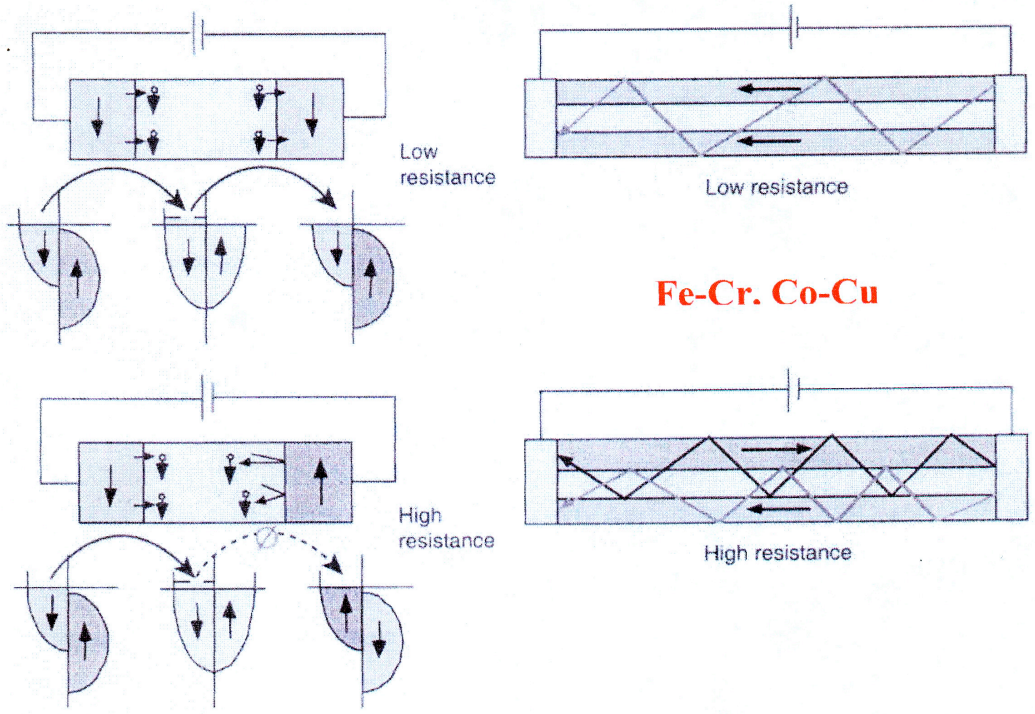

Search for materials with 100% polarization:

$$P = \frac{n_{\uparrow} - n_{\downarrow}}{n_{\uparrow} + n_{\downarrow}} = 1$$

Engineering a half metal ferromagntic material – $Co_{1-x}Fe_xS_2$

- CoS_2 Metallic ferromagnet
- FeS_2 Diamagnetic semiconductor
- $Co_{1-x}Fe_xS_2$ Half-Metallic Ferromagnet?

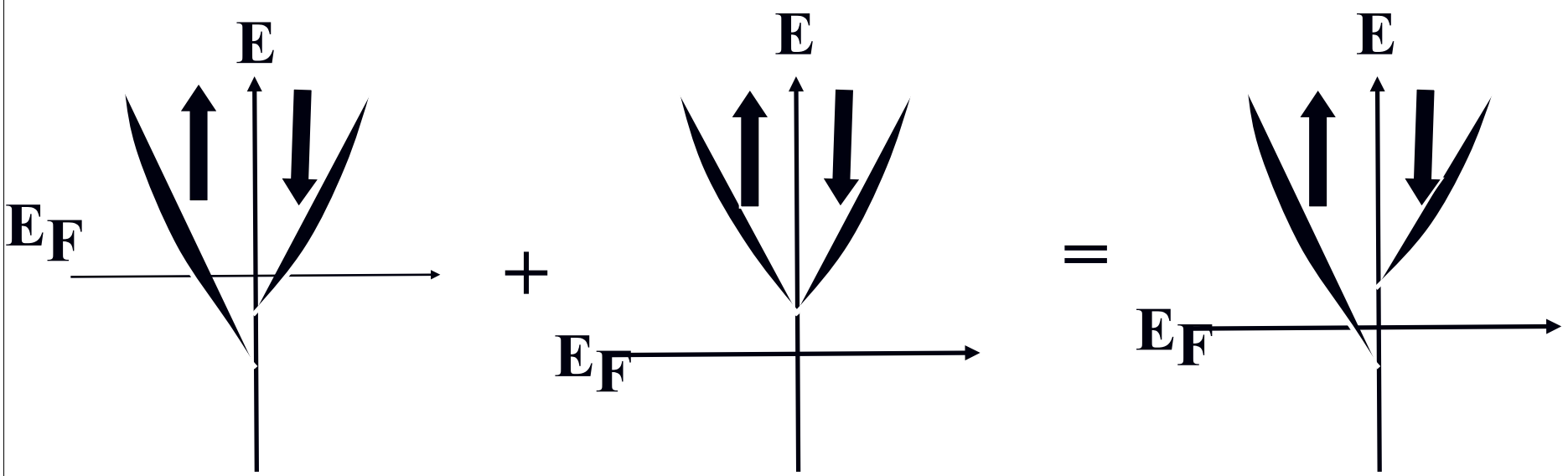

Electronic structure calculations

- **Pseudopotentials, plane-wave expansion, and the LSDA**

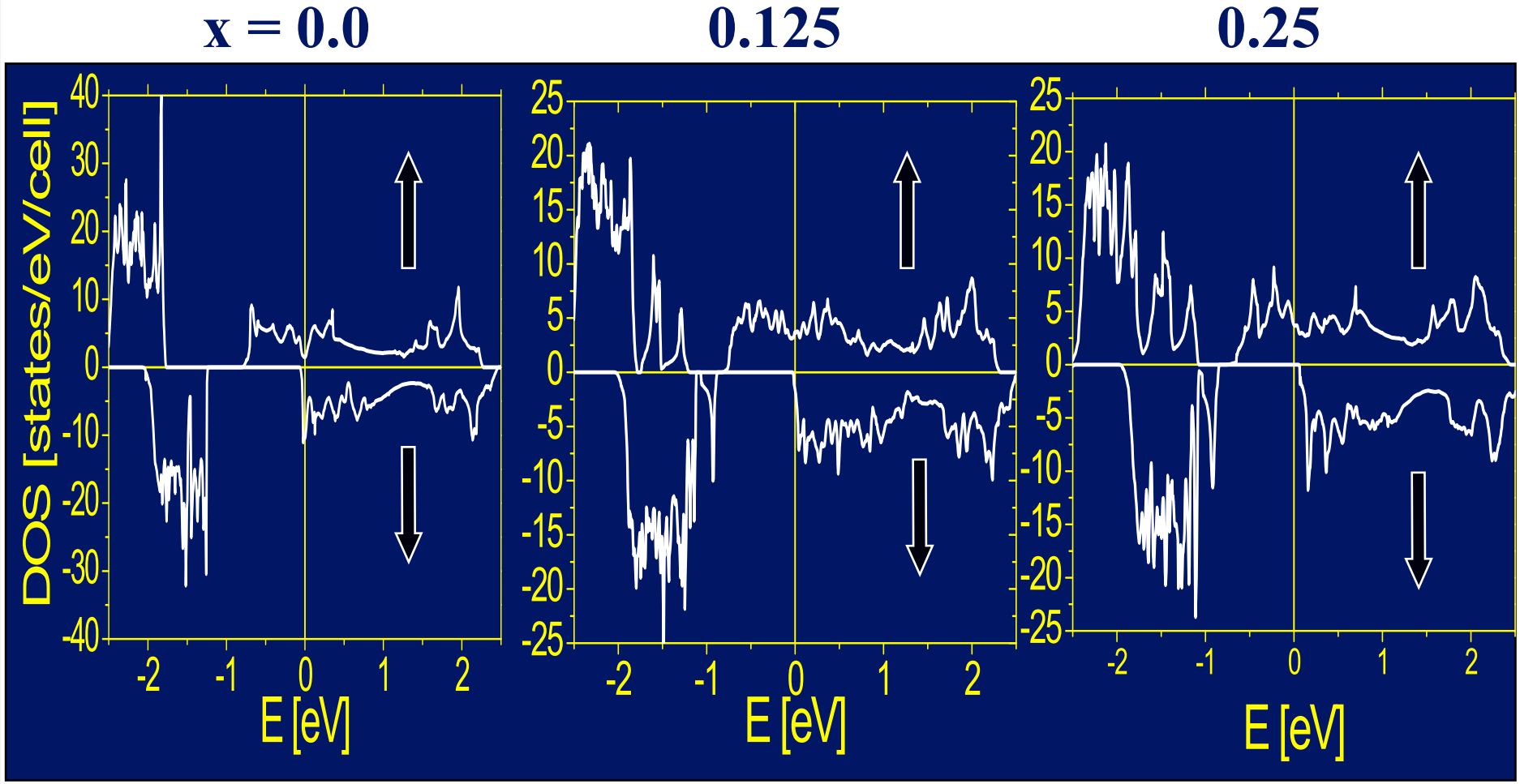

P = -70% **+ 40 %** **+100 %**

Wentzcovitch et al.

Spintronic materials are often made of dilute magnetic semiconductors alloyed with a magnetic element. These alloys are both ferromagnetic and semiconducting, opening the door to exciting "spintronics" applications - devices based on both electron charge and spin.

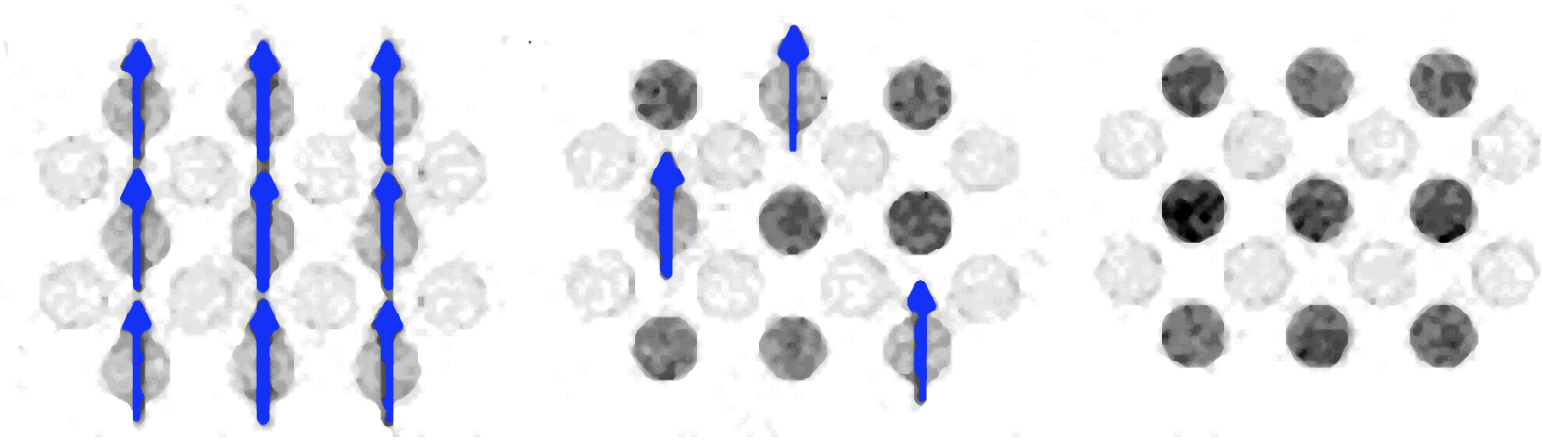

Magnetic

Dilute Magnetic

Non-magnetic

MnGaN: Role of Ga 3d States

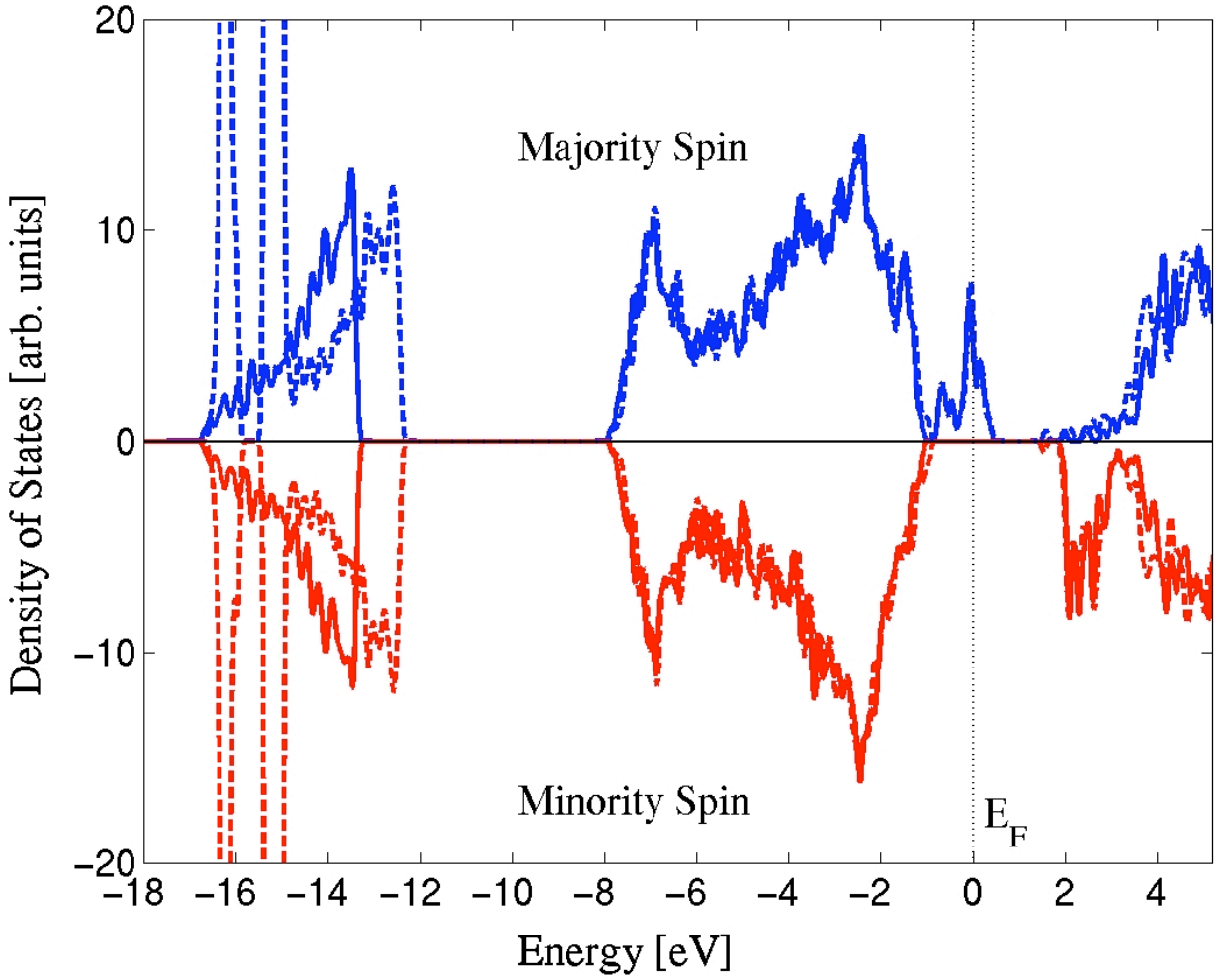

Dashed line with 3d state treated explicitly.

Key results:
-Valence band not polarized.
-State in the gap "half-metallic".
-Minority polarization in conduction band states.

Ga 3d and N 2s states do interact, but effect on band gap energy is minimal

Kronik, Jain and Chelikowsky

Growth Modes of Mn on Ge (100) and Ge (111) Surfaces

- Growth mechanisms, important but largely unexplored.
- Use pseudopotential-density functional theory to examine the growth of Mn on Ge surfaces
- Low Mn doses on Ge (100) initiates novel subsurface growth whereas Mn on the (111) surface can diffuse into the bulk via interstitial sites.

Kaxiras et al.

(100) Ge Surface

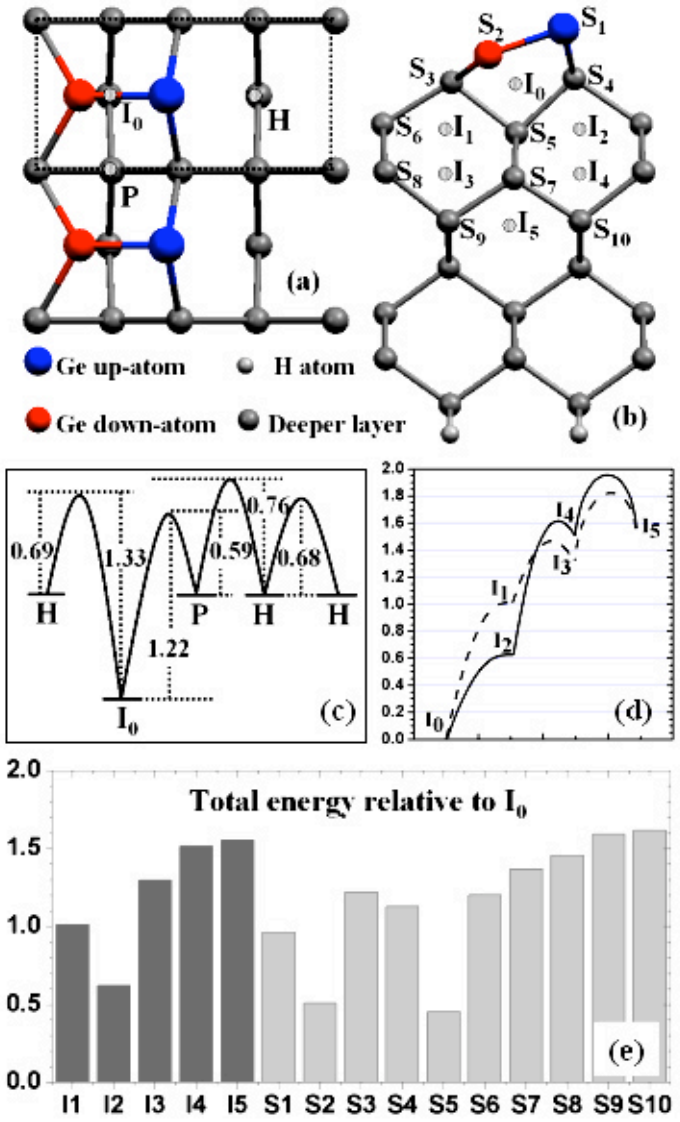

(111) Ge Surface

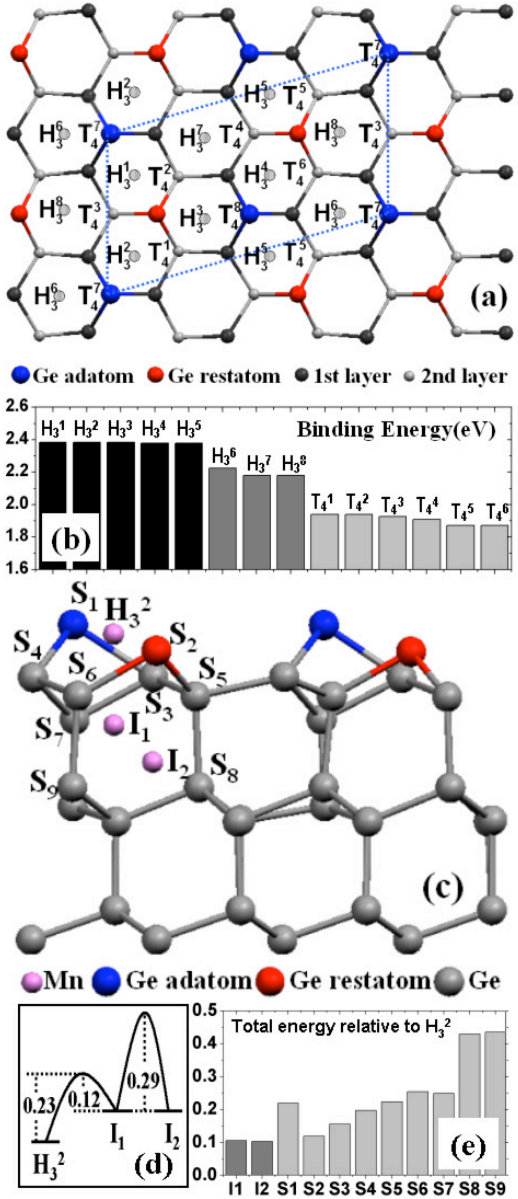

Quantum Dots: Optical and Magnetic Properties

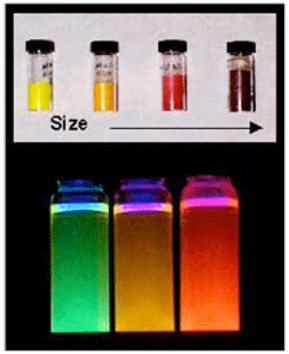

Examine the role of quantum confinement
- Profound effect on the optical properties of nanocrystal

Confinement should also have strong effect on spin-spin exchange.
- Study and manipulate a single spin in a semiconductor box.
- Serve as a model for spintronic materials.

Structure of Zn_mSe_m clusters

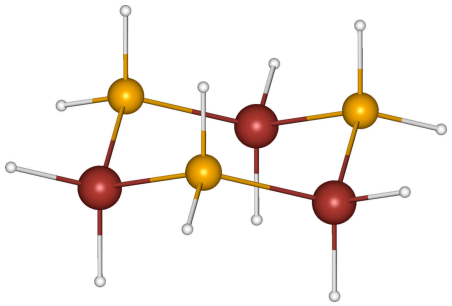

Zn_3Se_3

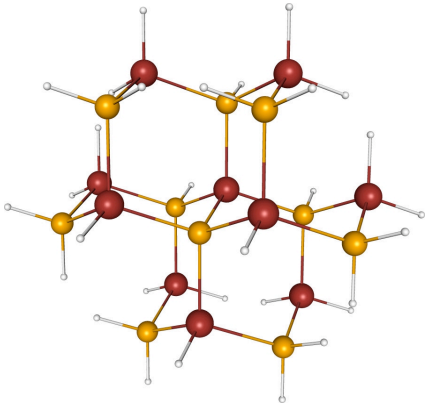

$Zn_{10}Se_{10}$

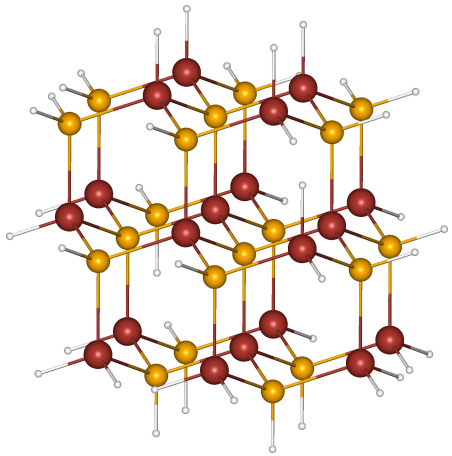

$Zn_{19}Se_{19}$

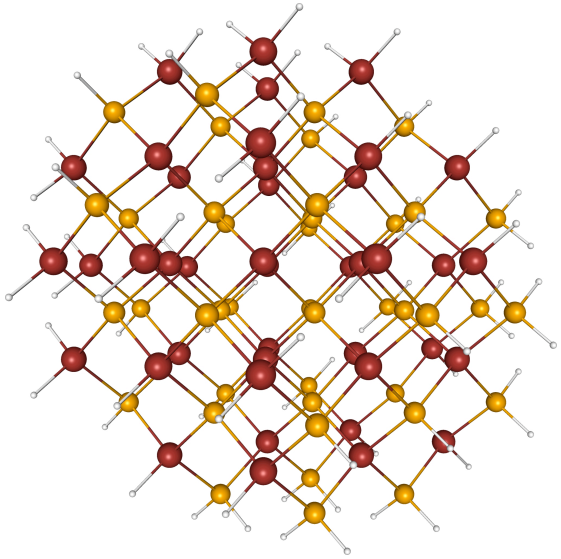

$Zn_{41}Se_{41}$

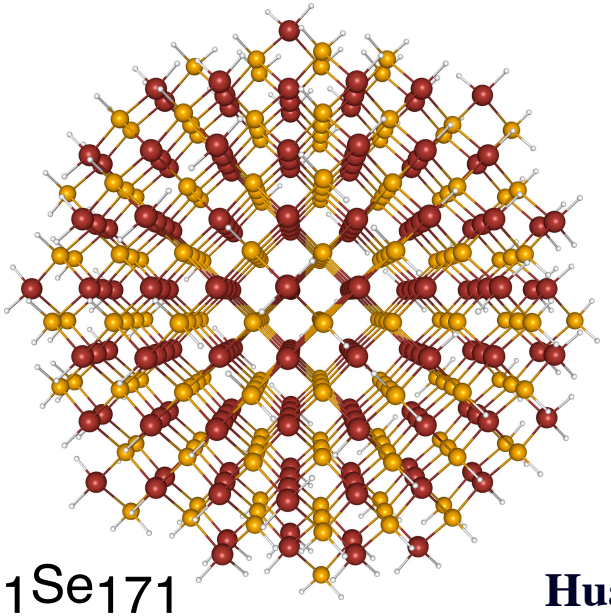

$Zn_{171}Se_{171}$

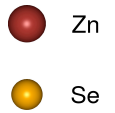

Huang and Chelikowsky

$MnZn_{18}Se_{19}$ quantum dots

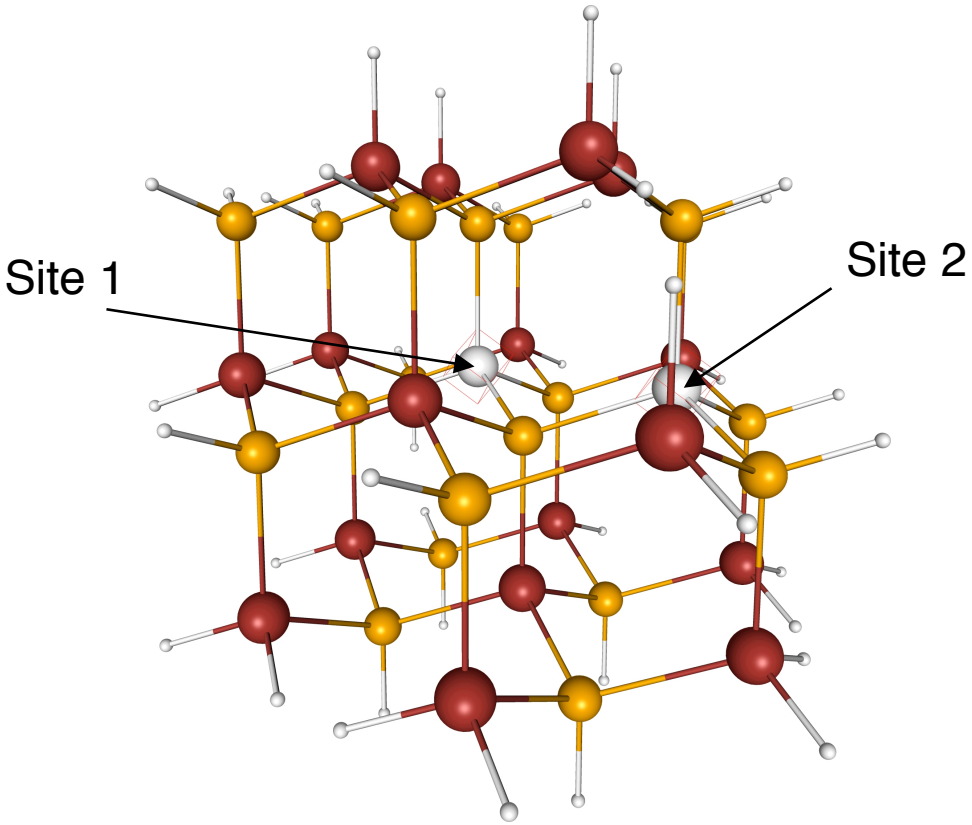

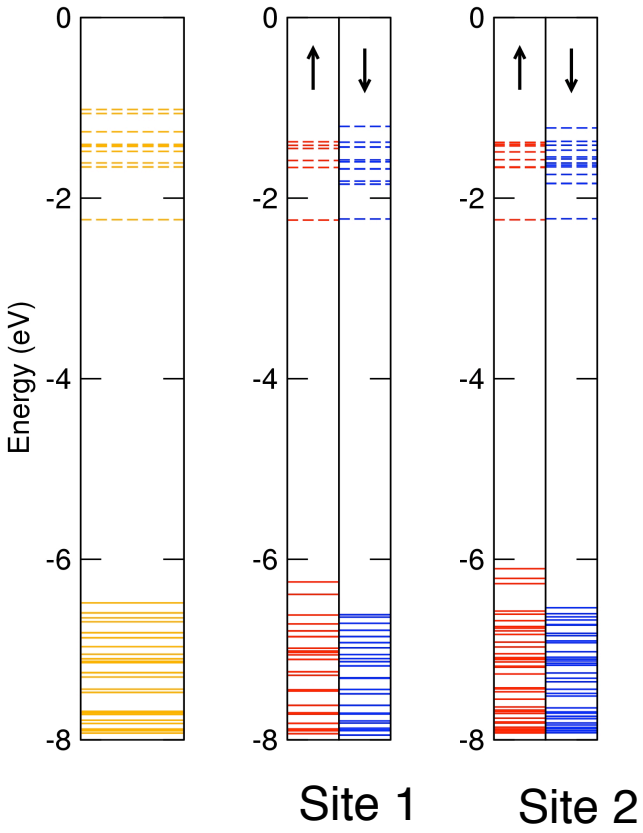

- Mn impurity in the ZnSe quantum dot has a high spin state
- The impurity levels are not sensitive to the impurity position in the cluster

Impurity state in the $MnZn_{18}Se_{19}$ quantum dot

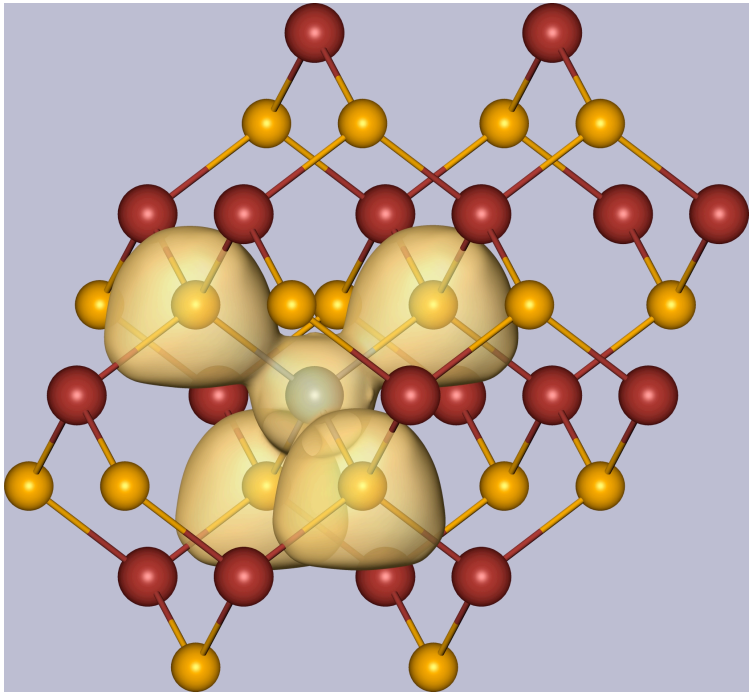

Isosurface of charge density in the vicinity of the Mn atom

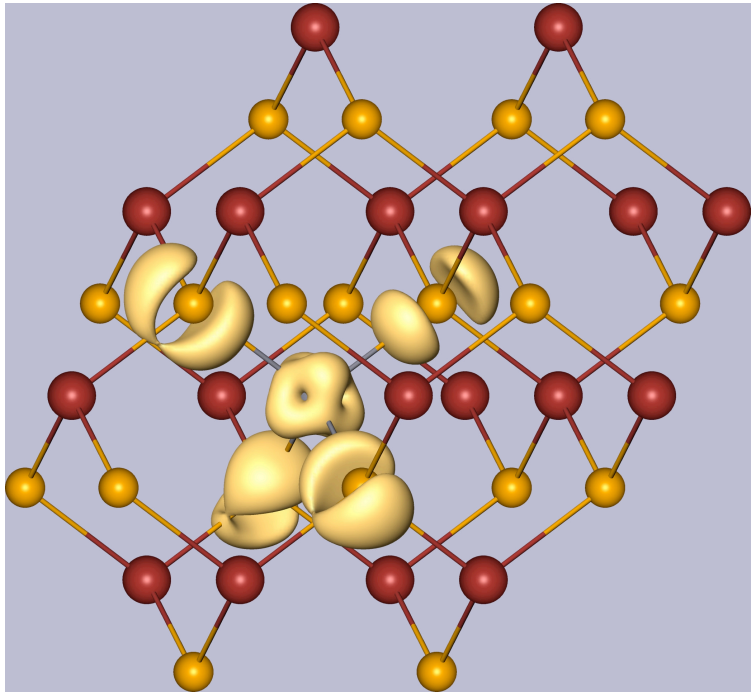

Isosurface of summation of wave function square of impurity levels

- Bonding between Mn and Se atoms
- Impurity levels are highly localized around Mn

Research on Numerical Algorithms for Materials

Institute for the Theory of Advanced Materials in Information Technology

Yousef Saad

University of Minnesota

Department of Computer Science and Engineering

NSF Division of Materials Research ITR Computational Workshop

UIUC, June 17-19, 2004

Numerical problems in DFT

- Original Schrödinger equation exceedingly complex.

- Density Functional Theory + Local Density Approximation + Pseudopotentials lead to "one-electron" model $\longrightarrow$ nonlinear eigenvalue problem

Main issues of interest:

- Solve the eigenvalue problem efficiently [specificity: large number of eigenvalues]

- Find alternatives [avoid eigenvectors, eigenvalues]

- Solve various related computational problems [TDDFT, computation of dielectric matrix, ...]

➨ Kohn-Sham equation

$$\left[-\frac{h^2}{2m}\nabla^2 + V_{tot}[\rho(r)]\right]\Psi(r) = E\Psi(r)$$

With

$$V_{tot} = V_{ion} + V_H + V_{xc}$$

- V_H = Hartree potential ➨ **Local**
- V_{xc} = Exchange & Correlation potential ➨ **Local**
- V_{ion} = Ionic potential ➨ **Non-Local**

➨ Electron Density:

$$\rho(r) = \Sigma_i^{occup} |\Psi_i(r)|^2$$

➨ Above problem can be viewed as a nonlinear eigenvalue problem.

Work on eigenvalue algorithms

Current focus:

(1) AMLS and related methods

(2) Block versions of restarted Lanczos

Motivation:

(1) Excellent success of AMLS in structural engineering. Similarity: large number of eigenvectors to compute

(2) Standard packages (ARPACK) do not easily take advantage of self-consistent loop. Also: not specialized for large number of eigenvalues.

Block-Lanczos – advantages

- Basic principle of the Block Lanczos algorithm: operate on block of b columns instead of only one column as in standard Lanczos.

Advantages:

- Can exploit a block of several initial guesses of eigenvectors
- Deals well with clustered or multiple ('degenerate') eigenvalues
- Can yield better cache performance (BLAS 3 instead of BLAS 2)

Issues:

- How to implement implicit restarts?
- Important to dynamically adapt block size

Automatic Multi-Level Substructuring

Origin: Extention of substructuring for eigenvalue problems.

Background: Domain decomposition. Let $A \in \mathbb{C}^{n \times n}$, Hermitian

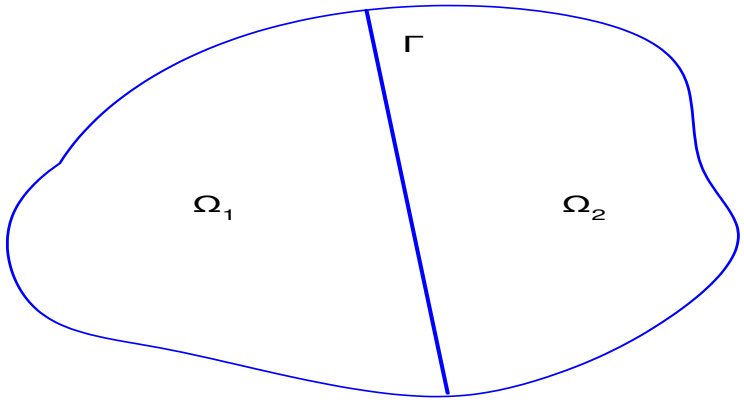

$$\rightarrow A = \begin{pmatrix} B & E \\ E^* & C \end{pmatrix} \quad B \in \mathbb{C}^{(n-p)\times(n-p)}$$

Note: B **is block-diagonal**

Main Reference:

J. K. Bennighof and R. B. Lehoucq, ***An automated multilevel substructuring method for eigenspace computation in linear elastodynamics***, **To appear in SIAM. J. Sci. Comput.**

Basic idea of the method for two levels

First step: eliminate the blocks E, E^*.

$$U = \begin{pmatrix} I & -B^{-1}E \\ 0 & I \end{pmatrix} \rightarrow U^*AU = \begin{pmatrix} B & 0 \\ 0 & S \end{pmatrix}; \quad S = C - E^*B^{-1}E.$$

Original problem is equivalent to $U^*AUu = \lambda U^*Uu \rightarrow$

$$\begin{pmatrix} B & 0 \\ 0 & S \end{pmatrix} u = \lambda \begin{pmatrix} I & -B^{-1}E \\ -E^*B^{-1} & M_S \end{pmatrix} u \; ; M_S = I + E^*B^{-2}E$$

Second step: neglect the coupling in right-hand side matrix:

$$Bv = \mu\, v$$

$$Sw = \eta\, M_S w.$$

➨ Compute a few of the smallest engenvalues of the above problem.

Third step: Build a 'good' subspace to approximate to eigenfunctions of original problem. The basis used for this projection is of the form

$$\left\{ \hat{v}_i = \begin{pmatrix} v_i \\ 0 \end{pmatrix} \quad i = 1, \ldots, m_B; \qquad \hat{w}_j = \begin{pmatrix} 0 \\ w_j \end{pmatrix} \quad j = 1, \ldots, m_S \right\},$$

where $m_B < (n-p)$ and $m_S < p$.

Then use this subspace for a Rayleigh-Ritz projection applied to

$$\begin{pmatrix} B & 0 \\ 0 & S \end{pmatrix} \begin{pmatrix} u^B \\ u^S \end{pmatrix} = \lambda \begin{pmatrix} I & -B^{-1}E \\ -E^* B^{-1} & M_S \end{pmatrix} \begin{pmatrix} u^B \\ u^S \end{pmatrix}$$

(Note: not the original problem.)

Final step: exploit recursion –

NOTE: algorithm does only one shot of descent - ascent (no iterative improvement).

Eigenvalue-free DFT

Recall:

$$\rho(r) = \sum_{j=1}^{occ} |\Psi_j(r)|^2$$

Main observation: **The eigenvectors are not really needed. When $\psi_j(r)$ is discretized w.r.t. r then the $\rho(r_i) \equiv \rho_{ii}$ is the diagonal entry of the 'functional density matrix'**

$$P(r,r') = \sum_{j=1}^{occ} \Psi_j(r)\overline{\Psi_j(r')} \quad \text{or} \quad P = VV^*, \quad V = [\psi_1, \ldots, \psi_{occ}]$$

➨ **'Order n methods' based on finding an approximation to P. Sparsity of P (in specific bases) is exploited.**

Approaches

$$P = f(H)$$

where f is a step function. Approximate f by, e.g., a polynomial

- Result: can obtain columns of P inexpensively via:

$$Pe_j \approx p_k(H)e_j$$

- Exploit sparsity of P (especially in planewave basis)- ideas of "probing" allow to compute several columns of P at once.

- Statistical approach: work of Hutchinson for estimating trace of a matrix [used in image processing] adapted to estimating diagonals.

- Many variants currently being investigated

TDLDA: Use of planewave bases and FFT

Recall :

$$K_{ij,kl} = \int_\Omega \left(\Psi_i(\mathrm{r}) \bar{\Psi}_j(\mathrm{r}) \frac{dV_{\mathbf{xc}}(\mathrm{r})}{d\rho(\mathrm{r})} + \Phi_{ij}(\mathrm{r}) \right) \Psi_k(\mathrm{r}) \bar{\Psi}_l(\mathrm{r}) d\mathrm{r}.$$

With $\triangle \Phi_{ij}(\mathrm{r}) = -4\pi \Psi_i \bar{\Psi}_j(\mathrm{r}).$

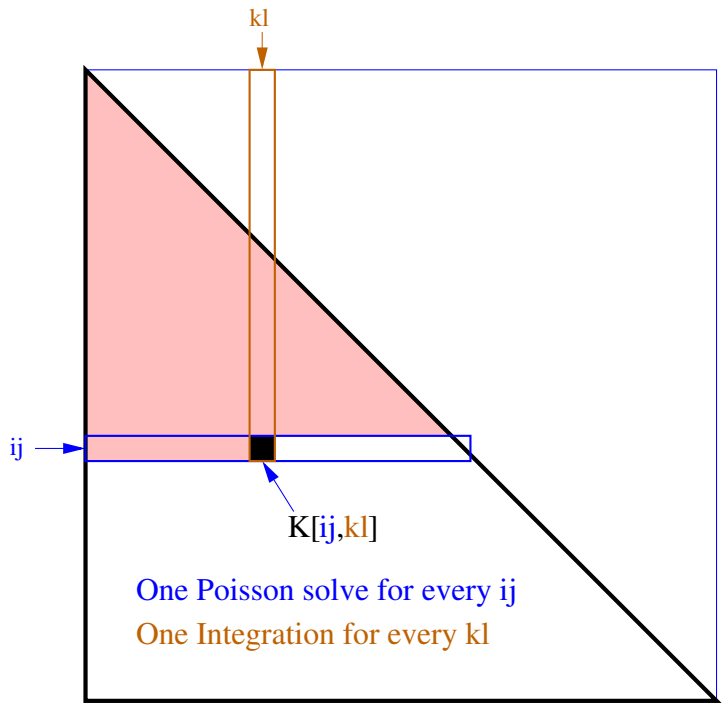

Coupling Matrix K

- Previous work [our group] : work in real space + use CG to solve Poisson's equation.

- Real space approach does not exploit specific features of the physics when solving Poisson's equation.

- Idea is to use FFTs: (In essence: Use "fast Poisson solvers")

- Expand each wavefunction in planewave basis:

$$\Psi_j(\mathrm{r}) = \sum_{\mathrm{l}} \psi_{\mathrm{l}}^j \exp i(\mathrm{l}.\mathrm{r}) \rightarrow \Phi_{ij}(\mathrm{r}) = 4\pi \sum_{(\mathrm{l},\mathrm{l}')\mathrm{l}\neq\mathrm{l}'} \frac{\psi_{\mathrm{l}}^i \bar{\psi}_{\mathrm{l}'}^j}{\|\mathrm{l}-\mathrm{l}'\|^2} e^{i(\mathrm{l}-\mathrm{l}').\mathrm{r}}.$$

- Many improvements can now be made. For example, in practice meaningful 'support' of $\psi_i\psi_j$ is small

$$\mathcal{F}(\Psi_i\bar{\Psi}_j)(\mathrm{k}) = \sum_{\mathrm{r}} e^{i\mathrm{k}.\mathrm{r}}(\Psi_i\bar{\Psi}_j)(\mathrm{r}) = \sum_{\mathrm{r}\,\in\,\mathbf{Supp}(\Psi_i\bar{\Psi}_j)} e^{i\mathrm{k}.\mathrm{r}}(\Psi_i\bar{\Psi}_j)(\mathrm{r}).$$

Results

- **Compare Real space code with planewave code for $Si34H36$**

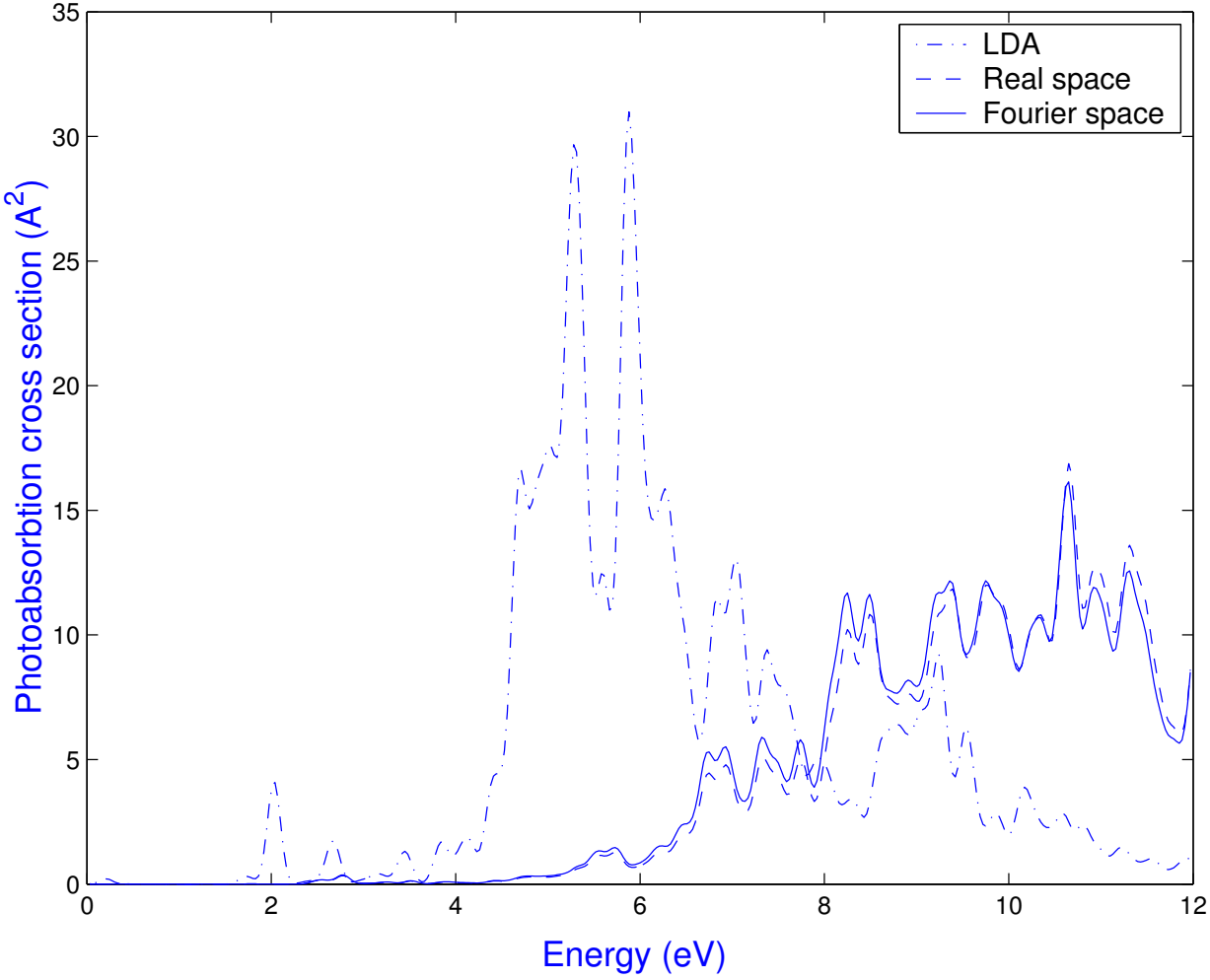

- Compare times for Real space code and planewave code [for $Si34H36$]

Method	Wall-Clock Time (hours)
Real Space Code	15:30
PW: Initial Implementation	3:30
PW: Optimized load balancing	2:30

Wall-clock time of the parallel TDLDA code using Fourier space and Real Space for the Si34H36 test case running on 8 processors

Note: Gain a factor of 5-6 wrt to optimized version of TDLDA code. Compound with another factor of 3-4 from original to optimized real-space code $\longrightarrow$ 15 to 24 faster than [Vasiliev et al. 2000]

- More to come!